Light Absorption and Electrical Characteristics of DUV-LED with Dual Superlattice Layer Growth

Chandra Prakash Singh
Dept. of Elec. Engg., IIT Jammu, Jammu 181221, India
2020ree2054@iitjammu.ac.in

Kankat Ghosh
Dept. of Elec. Engg., IIT Jammu, Jammu 181221, India
kankat.ghosh@iitjammu.ac.in

***Abstract*— This study investigates the effects of utilizing dual superlattice layer growth instead of a uniform p-AlGaN layer. The objective is to enhance acceptor doping efficiency, reduce absorption losses, and lower operating voltage. The results demonstrate significant improvements, including a 212% increase in light output power, a 144% increase in internal quantum efficiency, and a 16% reduction in efficiency droop, accompanied by a substantial reduction in absorption losses.**

Keywords— III-Nitride, Light absorption, Quantum Efficiency.

I. Introduction

AlGaN-based deep ultraviolet light-emitting diodes (DUV LEDs) emitting around 275 nm have attracted significant attention for their effectiveness in deactivating coronaviruses such as SARS-CoV-2, SARS, MERS, and various other pathogens. Despite their market potential, DUV LEDs currently have an external quantum efficiency (EQE) below 10%, which hinders their ability to replace traditional mercury-based lamps. A major challenge in improving the EQE of DUV LEDs is the inefficiency of acceptor doping, which leads to a low concentration of hole carriers in the active region, necessitating higher voltage operation. Using low Al-content in p-AlGaN heterostructures can support low-voltage operation due to reduced series resistance. However, this approach can drastically reduce light extraction efficiency (LEE) by up to 90% because of strong UV-C absorption in the p-AlGaN heterostructures, significantly lowering the EQE. Conversely, higher Al-content in the p-AlGaN heterostructure improves transparency but requires higher voltage operation, consequently reducing wall plug efficiency (WPE). Therefore, achieving high EQE in DUV LEDs requires optimizing the Al-content in the p-AlGaN heterostructure by balancing the reduction of absorption losses with the limitation of increases in operating voltage.

This study proposes an optimized approach utilizing a dual superlattice (DSL) growth strategy to enhance acceptor doping and reduce absorption losses in DUV-LEDs. The engineering involves replacing the uniform p-AlGaN hole injection layer (HIL) with a DSL grown on the electron-blocking layer (EBL). All devices investigated in this study were simulated using Nextnano software and feature identical n-AlGaN layers, active regions, and EBLs [3].

II. Device Structure

Fig. 1 represents the schematic of a typical DUV-LED structure previously reported and experimentally validated by Hu et al. [4], along with the engineered device structures. The reference (LED-R) includes a 3 µm thick n-$Al_{0.6}Ga_{0.4}N$ layer,

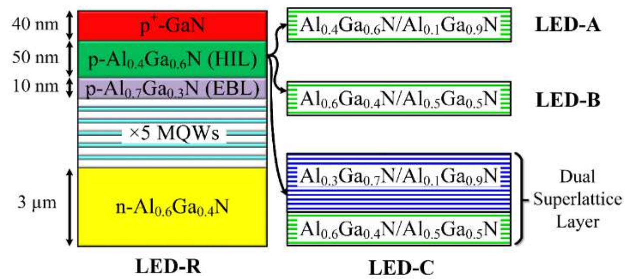

Fig. 1. Reference experimental device structure (LED-R) with engineered device structure of DUV LED emitting wavelength of ~273 nm.

followed by five pairs of multiple quantum wells (MQWs), each consisting of a 2 nm thick $Al_{0.45}Ga_{0.55}N$ quantum well and a 14 nm thick $Al_{0.57}Ga_{0.43}N$ barrier. The p-heterostructure comprises a 10 nm thick p-$Al_{0.7}Ga_{0.3}N$ EBL, a 50 nm thick p-$Al_{0.4}Ga_{0.6}N$ HIL, and a 40 nm thick p^+-GaN contact layer. The size of the LED-R is 762 × 762 µm², and it emits light at a wavelength of ~273 nm. The engineered LEDs (LED-A, LED-B, and LED-C) feature identical n-region, MQWs, and EBL as the LED-R. However, LED-A and LED-B incorporate a short-period (×5) SL layer instead of a uniform p-AlGaN HIL. LED-A consist of $Al_{0.4}Ga_{0.6}N$ (2.5 nm)/$Al_{0.1}Ga_{0.9}N$ (2.5 nm), and LED-B consists of $Al_{0.6}Ga_{0.9}N/Al_{0.5}Ga_{0.5}N$. In contrast, LED-C utilizes a dual SL layer instead of uniform HIL, with a long-period (×20) SL of $Al_{0.3}Ga_{0.7}N$(2.5 nm)/$Al_{0.1}Ga_{0.9}N$(2.5 nm), is grown on the short-period SL layer having the same Al-composition as in LED-B, as illustrated in Fig. 1.

III. Results And Discussion

The electroluminescence (EL) spectra calculated at 20 A/cm² for all the structures are shown in Fig. 2 (a). All DUV-LEDs exhibit a single emission peak around 273 nm, with the engineered LEDs demonstrating superior EL intensity compared to LED-R. Additionally, these LEDs have relatively smaller full-width half-maxima (FWHM) values: 12.58 nm for LED-A, 11.40 nm for LED-B, and 10.45 nm for LED-C, compared to 13.23 nm for LED-R. As shown in Fig. 2 (b), replacing the uniform Al-composition HIL significantly improves the hole carrier concentrations within the active region. This improvement results from the decrease in the effective valence band potential barrier height at the corresponding EBL, decreasing from 0.44 eV for LED-R to 0.32 eV for LED-B and 0.28 eV for LED-C. Notably, the hole concentration in LED-C exhibits an improvement compared to LED-B. This enhancement can be attributed to the DSL utilized in LED-C,

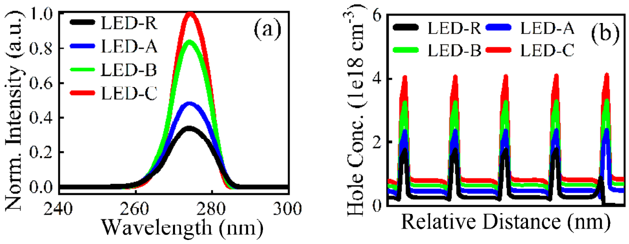

Fig. 2. (a) Calculated EL-spectra, and (b) The distribution of hole concentration of all the structure at 20 A/cm².

which enhances hole injection efficiency through more effective intra-band tunnelling processes and thermionic emission. On the other hand, a significant enhancement in electron concentration is observed, which is attributed to the increase in the effective conduction band potential barrier height at the corresponding EBL, rising from 0.69 eV for LED-R to 0.80 eV for LED-B and LED-C. Thus, the significantly enhanced electron-blocking capabilities in LED-A/B/C lead to a substantial reduction in electron leakage into the p-region. Additionally, this leads to the suppression of undesirable non-radiative recombination of holes with leaked electrons in the p-region [5].

The combined enhanced hole and electron concentration contribute to a more significant radiative recombination rate. This increase in the radiative recombination rate leads to improved light output power (LOP) and internal quantum efficiency (IQE), as evidenced in Fig. 3. Specifically, the LOP is enhanced by 67%, 147%, and 212% for LED-A, LED-B, and LED-C, respectively, compared to LED-R at 20 A/cm². Similarly, the maximum IQE is improved by 55%, 105%, and 144% for LED-A, LED-B, and LED-C, respectively, compared to LED-R. Additionally, the efficiency droop at 80 A/cm² decreases from 65% for LED-R to 43%, 32%, and 16% for LED-A, LED-B, and LED-C, respectively.

As depicted in Fig. 4 (a), the absorption spectra reveal negligible absorption for all DUV-LEDs above the peak emission wavelength of 273 nm, leading to homogeneous broadening in the experimentally measured EL-spectra within this range. However, below the peak emission wavelength, we anticipate the appearance of inhomogeneous broadening in the experimentally measured EL-spectra due to varying levels of absorption intensity. The introduction of the short-period SL in LED-A reduces absorption intensity compared to LED-R, which has the same Al-composition (40%) but uniform AlGaN layer.

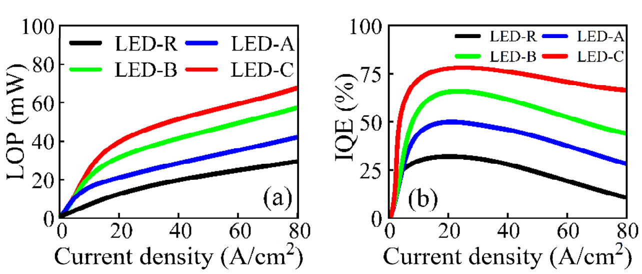

Fig. 3. (a) LOP, and (b) IQE plot of all the structures at various injection currents density ranging from 0 to 80 A/cm².

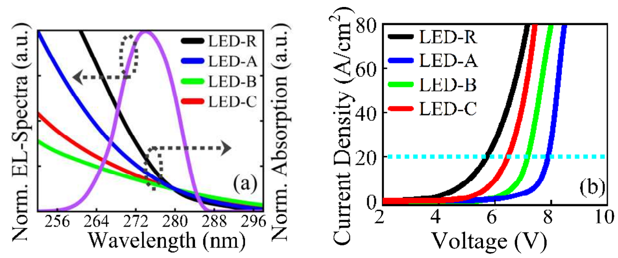

Fig. 4. (a) Normalized absorption spectrum of the entire DUV-LED heterostructure for all DUV-LEDs, plotted against the calculated EL emission spectra of the LED-C (purple-line). This absorption spectrum is normalized at 280 nm, assuming negligible absorption for all DUV-LEDs, and (b) The distribution of current density with voltage.

This reduction is primarily due to the SL structure in LED-A, forming energy bands with a larger bandgap than uniform AlGaN regions with the same compositions, thus enhancing transparency to the emission wavelength. Furthermore, LED-B, with higher average Al-compositions than LED-A, exhibits much lower absorption intensity, indicating better transparency. Notably, LED-C with a DSL shows slightly higher absorption intensity than LED-B due to the reduction in average Al-composition with the growth of long-period SL having low Al-composition. However, this long-period SL significantly reduces the operating voltage compared to LED-B, as evidenced in Fig. 4 (b). Specifically, the operating voltage to reach (@ 20A/cm²) is reduced by 9.5%, and 18.2% for LED-B and LED-C, respectively, compared to LED-A.

IV. Conclusion

In summary, this study demonstrates that incorporating a dual SL (long-period $Al_{0.3}Ga_{0.7}N/Al_{0.1}Ga_{0.9}N$ on short-period SL of $Al_{0.6}Ga_{0.9}N/Al_{0.5}Ga_{0.5}N$) in DUV-LEDs significantly enhances both carrier injection, reduces light absorption losses and operating voltage, and thus improves WPE and IQE. These findings underscore the effectiveness of the DSL approach in optimizing DUV-LED performance.

Acknowledgment

This work received support from the FIST scheme of DST (SR/FST /ET-II/2021/814), the Government of India, and the Indian Institute of Technology Jammu.

References

[1] C. Zhang *et al*. "Recent progress on AlGaN based deep ultraviolet light-emitting diodes below 250 nm," Crystals, vol. 12, no. 12, p. 1812, Dec. 2022.

[2] Y. Kang et al., "Efficiency droop suppression and light output power enhancement of deep ultraviolet light-emitting diode by incorporating inverted-V-shaped quantum barriers," IEEE Trans. Electron Devices, vol. 67, no. 11, pp. 4958–4962, Nov. 2020.

[3] H. K. Cho *et al*., "Highly Reflective p-Contacts Made of Pd-Al on Deep Ultraviolet Light-Emitting Diodes," in IEEE Photonics Technology Letters, vol. 29, no. 24, pp. 2222-2225, 15 Dec.15, 2017.

[4] J. Hu *et al*., "Enhanced performance of AlGaN-based deep ultraviolet light-emitting diodes with chirped superlattice electron deceleration layer," *Nanosc. Res. Lett.*, vol. 14, no. 1, pp. 1–8, Dec. 2019.

[5] C. P. Singh, and K. Ghosh, "Lower Current Density Driven InGaN/GaN Micro-LED with Improved Quantum Efficiency," *Optik*, pp. 171664, 2024.